NATIONAL AERONAUTICS AND SPACE ADMINISTRATION

TECHNICAL REPORT
R-31

ANALYSIS OF TURBULENT FLOW AND HEAT TRANSFER IN NONCIRCULAR PASSAGES

By ROBERT G. DEISSLER and MAYNARD F. TAYLOR

1959

For sale by the Superintendent of Documents, U.S. Government Printing Office, Washington 25, D.C. Yearly subscription, $10: foreign, $13; single copy price varies according to size. ---------- Price 30 cents

TECHNICAL REPORT R-31

ANALYSIS OF TURBULENT FLOW AND HEAT TRANSFER IN NONCIRCULAR PASSAGES

By ROBERT G. DEISSLER and MAYNARD F. TAYLOR

Lewis Research Center
Cleveland, Ohio

TECHNICAL REPORT R-31

ANALYSIS OF TURBULENT FLOW AND HEAT TRANSFER IN NONCIRCULAR PASSAGES [1]

By Robert G. Deissler and Maynard F. Taylor

SUMMARY

Previous work on turbulent heat transfer and flow in tubes was generalized and applied to flow in noncircular passages of equilateral triangular and square cross section. Expressions for eddy diffusivity that had been verified for flow and heat transfer in tubes were assumed to apply in general along lines normal to a wall. Velocity distributions, wall shear-stress distributions, and friction factors, as well as wall heat-transfer distributions, wall temperature distributions, and average heat-transfer coefficients, were calculated. In addition, results from a previous analysis for axial flow between rods were compared with new experimental data. For calculating wall temperature distributions, uniform heat generation in the passage wall and uniform heat transfer at the outer surface were assumed. The application of the results is restricted to moderately small peripheral wall temperature variations. Calculations were made for Reynolds numbers from 20,000 to 900,000 and Prandtl numbers from 0.73 to 300.

Results show that velocities, shear stresses, and heat transfer in the region near the corner were lower than average values and were zero at the corner. Friction factors and average Nusselt numbers were lower than in a tube.

INTRODUCTION

Until recently, most analyses for flow and heat transfer in passages were confined to circular tubes or to parallel plates. Those passages were analyzed extensively because of their importance in technical applications and because their simplicity makes them amenable to analysis.

In recent years the problems associated with the use of noncircular passages in heat exchangers have become important. In reference 1, wall temperature distributions for turbulent flow in rectangular and triangular ducts were calculated by using experimental velocity distributions and average heat-transfer coefficients, together with an assumed similarity of the wall heat-transfer and wall shear-stress variations; no attempt was made to calculate either the heat-transfer coefficients or the velocity and temperature distributions in the fluid field. Some calculations of velocity and shear-stress distributions in corners are reported in reference 2.

As a part of an investigation being conducted at the Lewis Research Center on heat transfer and flow in passages of various shapes, turbulent axial flow between rods and in eccentric annuli was analyzed in references 3 and 4. In the present investigation, the calculations were carried out for flow in passages having square and equilateral triangular cross sections. As in the previous analyses, expressions for eddy diffusivity that had been verified for flow and heat transfer in tubes were assumed to apply in general along lines normal to a wall. This assumption, although appearing to be reasonable, should of course be checked experimentally. Also, the peripheral temperature variation was assumed to be small compared with the variation of temperature across the passage.

[1] Supersedes NACA Technical Note 4384 by Robert G. Deissler and Maynard F. Taylor, 1958.

BASIC EQUATIONS AND ASSUMPTIONS

The differential equations for fully developed flow, shear stress, and heat transfer can be written in the following form:

$$\tau=(\mu+\rho\epsilon)\frac{du}{dy} \tag{1}$$

$$q=-(k+\rho c_p\epsilon_h)\frac{dt}{dy} \tag{2}$$

where ϵ and ϵ_h are the eddy diffusivities for momentum and heat transfer, respectively, the values for which depend on the amount and kind of turbulent mixing at a point. (All symbols are defined in appendix A.) In these equations, y is taken as the perpendicular distance from the wall, and τ and q are measured in planes parallel to the wall. Equations (1) and (2) can be considered as definitions of ϵ and ϵ_h. They can be written in dimensionless form as:

$$\frac{\tau}{\tau_0}=\left(\frac{\mu}{\mu_0}+\frac{\rho}{\rho_0}\frac{\epsilon}{\mu_0/\rho_0}\right)\frac{du^+}{dy^+} \tag{3}$$

$$\frac{q}{q_0}=\left(\frac{k}{k_0}\frac{1}{Pr_0}+\frac{\rho}{\rho_0}\frac{c_p}{c_{p_0}}\alpha\frac{\epsilon}{\mu_0/\rho_0}\right)\frac{dt^+}{dy^+} \tag{4}$$

where the subscript 0 refers to values at a wall and the properties in the definitions of u^+, y^+, and t^+ are evaluated at the wall.

EXPRESSIONS FOR EDDY DIFFUSIVITY

In order to use equations (3) and (4), the eddy diffusivity ϵ must be evaluated for each part of the flow. As in reference 5, in the region away from the wall the mechanism for turbulent transfer is assumed dependent only on the velocities in the vicinity of the point measured relative to the point, or on the space derivatives of the velocity. In the region close to the wall, the turbulence is assumed dependent on quantities measured relative to the wall, that is, on u and y and on the kinematic viscosity μ/ρ. On the basis of dimensional analysis and simplicity, it is assumed in reference 5 that, for the region close to the wall ($y^+<26$),

$$\epsilon=n^2uy\left(1-e^{-\frac{n^2uy}{\nu}}\right) \tag{5}$$

where the constant n has the experimentally determined value 0.124.[2]

In the region away from the wall ($y^+>26$), ϵ is assumed to be dependent on the relative velocities in the neighborhood of the point. From a Taylor's series expansion for u as a function of y and z,

$$\epsilon=f\left(\frac{\partial u}{\partial y},\frac{\partial^2 u}{\partial y^2},\ldots,\frac{\partial u}{\partial z},\frac{\partial^2 u}{\partial z^2},\frac{\partial^2 u}{\partial z\partial y}\ldots\right)$$

where y and z are measured in normal directions in the cross section of the passage. Since, in the case of flow through a tube or between parallel plates, the velocity-gradient line is a line that at each point is normal to a constant-velocity line, the derivatives in the z direction are zero. For flow in noncircular passages, the velocity-gradient lines near a wall are also normal to the surface but are usually curved in the center part of the passage. Inasmuch as the greatest changes of velocity with respect to distance take place in layers near the wall, the effect of the derivatives with respect to z will be neglected. It seems reasonable to expect that near the center of the flow passage the effect of the derivatives with respect to z would be to increase the turbulence and flatten the profile in that region. However, the normal turbulent profile (derivatives with respect to z absent) is already very flat in that region, so that the increased turbulence should not produce significant changes in the values of the velocities. Therefore, the expression for ϵ for $y^+>26$, obtained by using dimensional analysis, is

$$\epsilon=\kappa^2\frac{(du/dy)^3}{(d^2u/dy^2)^2} \tag{6}$$

where κ has the experimental value 0.36 (ref. 6); this is the von Kármán expression.

FURTHER ASSUMPTIONS

In order to integrate equations (3) and (4), the following assumptions are made, in addition to

[2] The quantity in parentheses in equation (5) becomes important only for heat transfer at Prandtl numbers appreciably greater than 1. For Prandtl numbers on the order of 1 or less, or for the calculation of velocity profiles, $\epsilon=n^2uy$ (the value of n differs from that in eq. (5)) and is a good approximation for the region close to the wall (ref. 6).

those concerning the eddy diffusivity (eqs. (5) and (6)):

(1) The fluid properties are considered constant. The analysis could be carried out for variable properties, but the complexity would be increased.

(2) The eddy diffusivities for momentum ϵ and heat transfer ϵ_h are equal (the ratio $\alpha=1$). Previous analyses for flow in tubes based on this assumption yielded heat-transfer coefficients that agreed with experiment (refs. 5 and 7). At low Reynolds or Peclet numbers ($Pe=RePr$), α appears to be a function of Peclet number (ref. 8); but for Reynolds numbers above 15,000, as in the present analysis, α is nearly constant for gases and for fluids with Prandtl numbers greater than 1.

(3) Along lines normal to a wall, the variations of the shear stress τ and heat transfer per unit area q have a negligible effect on the velocity and temperature distributions. It is shown in figure 12 of reference 7 that the assumption of a linear variation of shear stress and heat transfer across a tube (τ or $q=0$ at passage center) gives very nearly the same velocity and temperature profiles as those obtained by assuming uniform shear stress and heat transfer across the passage.

(4) The molecular shear-stress and heat-transfer terms in equations (3) and (4) can be neglected in the region away from the wall ($y^+>26$) (ref. 7, fig. 14).

GENERALIZED VELOCITY AND TEMPERATURE DISTRIBUTION

With the foregoing assumptions, equations (3) and (4) were integrated as in reference 5. The results are reproduced in figures 1 and 2. These curves give the relations of u^+, y^+, and t^+ used in the following calculations for flow in noncircular passages.

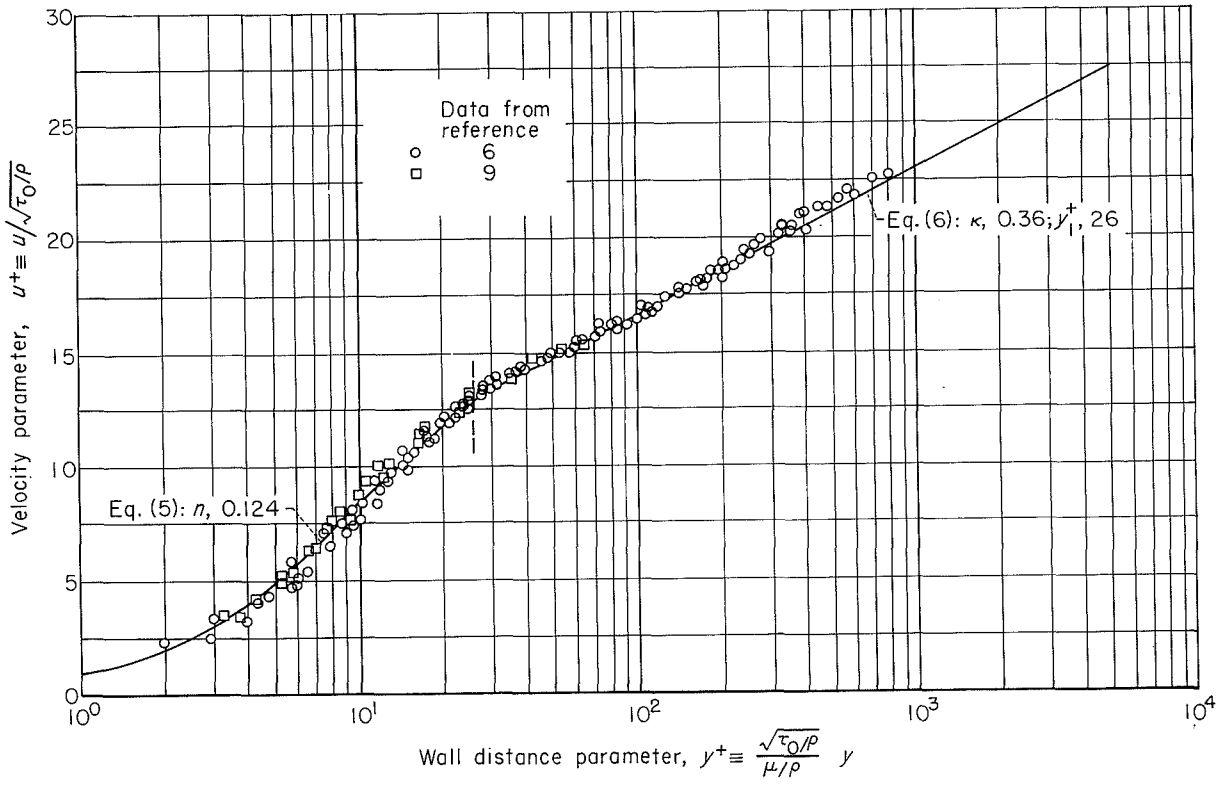

FIGURE 1.—Generalized velocity distribution for adiabatic turbulent flow. (Vertical dashed line is dividing line between eqs.)

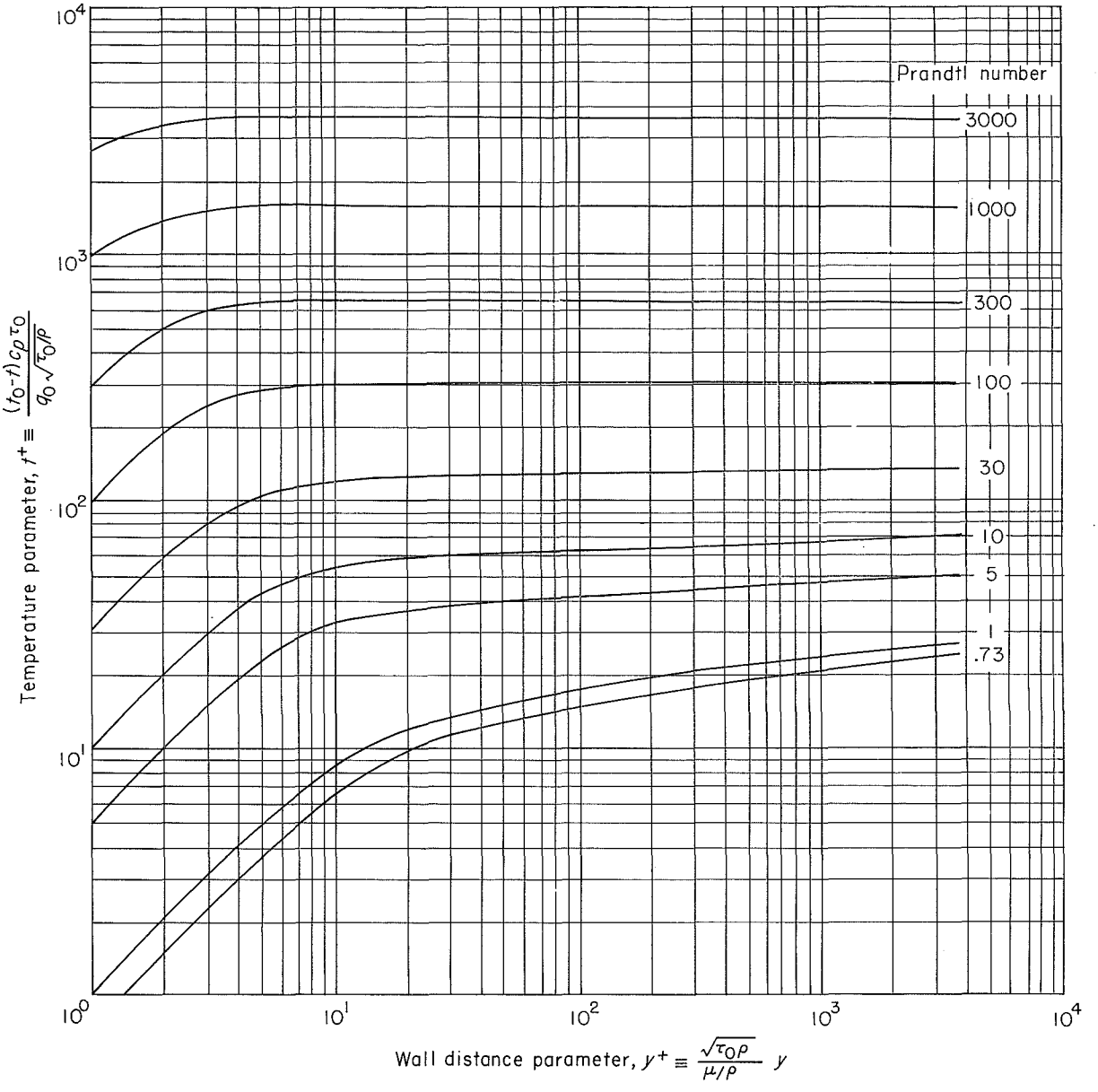

FIGURE 2.—Generalized temperature distributions for various Prandtl numbers.

CALCULATION OF VELOCITY DISTRIBUTIONS FOR FLOW IN NONCIRCULAR PASSAGES

For applying the relation between u^+ and y^+ in figure 1 to the calculation of velocity distributions for noncircular passages, an iterative procedure must be used, inasmuch as the lines of velocity gradient (lines normal to constant-velocity lines) are unknown at the outset. A typical flow passage of the type considered is shown in the following sketch.

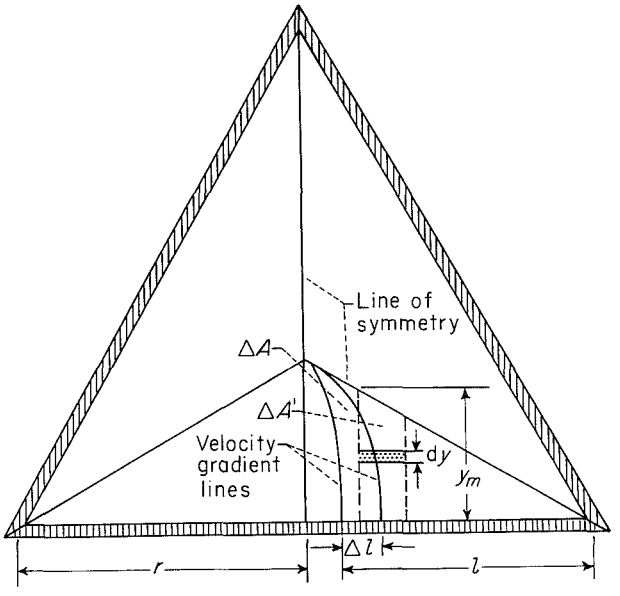

Sketch

The first step in obtaining the velocity distribution is to draw the line of symmetry; the velocities on either side of this line are lower than the velocities on the line. In the present case, the line can be drawn immediately from symmetry considerations, as shown in the sketch. The next step is to draw assumed velocity-gradient lines. By using these assumed velocity-gradient lines, lines of constant velocity can be calculated, as will be shown. A new and more accurate set of velocity-gradient lines can then be drawn, inasmuch as they must be normal to the constant-velocity lines. With a little practice, the velocity-gradient lines can be estimated quite accurately the first time, so that usually the iterative procedure need not be used more than once or twice.

CALCULATION OF LINES OF CONSTANT VELOCITY

For calculating velocities at various points in the passage, it is convenient to define the following velocity parameter:

$$u^{++} \equiv \frac{u}{\sqrt{\frac{-r\ \mathrm{d}p/\mathrm{d}x}{\rho}}} \tag{7}$$

This parameter is used in place of u^+ because the shear stress in the definition of u^+ varies with position. Equation (7) can be written in terms of quantities that can be calculated as

$$u^{++} = \frac{u^+ y_m^+}{r^{++} \frac{y_m}{r}} \tag{7a}$$

where

$$u^+ = F(y^+) = F\left(\sqrt{\frac{\tau_0/\rho}{\mu/\rho}}\,\frac{y_m}{y_m}\,y\right) = F\left(\frac{y}{y_m}\,y_m^+\right) \tag{8}$$

The function F is obtained from the relation between u^+ and y^+ in figure 1. The parameter r^{++} is a type of Reynolds number and is assigned an arbitrary value. In order to calculate y^+, a force balance is written on the element ΔA in the preceding sketch. The forces on the element are the shear force acting on Δl and the pressure forces acting on the faces of the element. There are no shear forces acting on the velocity-gradient lines because the normal velocity derivatives are zero along those lines. Writing a force balance on the element gives

$$\tau_0 = -\frac{\Delta A}{\Delta l}\left(\frac{\mathrm{d}p}{\mathrm{d}x}\right) \tag{9}$$

where the pressure gradient $\mathrm{d}p/\mathrm{d}x$ is uniform over the annulus because the flow is fully developed. Substituting equation (9) into the definition of y_m^+ results in

$$y_m^+ = \sqrt{\frac{\Delta A/\Delta l}{r}}\,r^{++} \frac{y_m}{r} \tag{10}$$

where ΔA, Δl, y_m, and r are measured from a figure similar to the preceding sketch and r^{++} is a parameter. If, for a specified value of r^{++}, a given line normal to the surface is considered, the value of y/y_m for a given u^{++} can be calculated by using equations (10), (7a), and (8) in that order.

By carrying out the calculation for various lines normal to the surface, lines of constant velocity (constant u^{++}) can be obtained. As mentioned previously, new and more accurate velocity-gradient lines are next drawn so as to intersect the constant-velocity lines at right angles. The calculation is then repeated with the new velocity-gradient lines.

CALCULATED VELOCITY DISTRIBUTIONS

Several velocity distributions for flow in equilateral triangular and in square passages, calculated by the method described, are shown in figure 3. The calculations were carried out for several Reynolds numbers, but the effect of

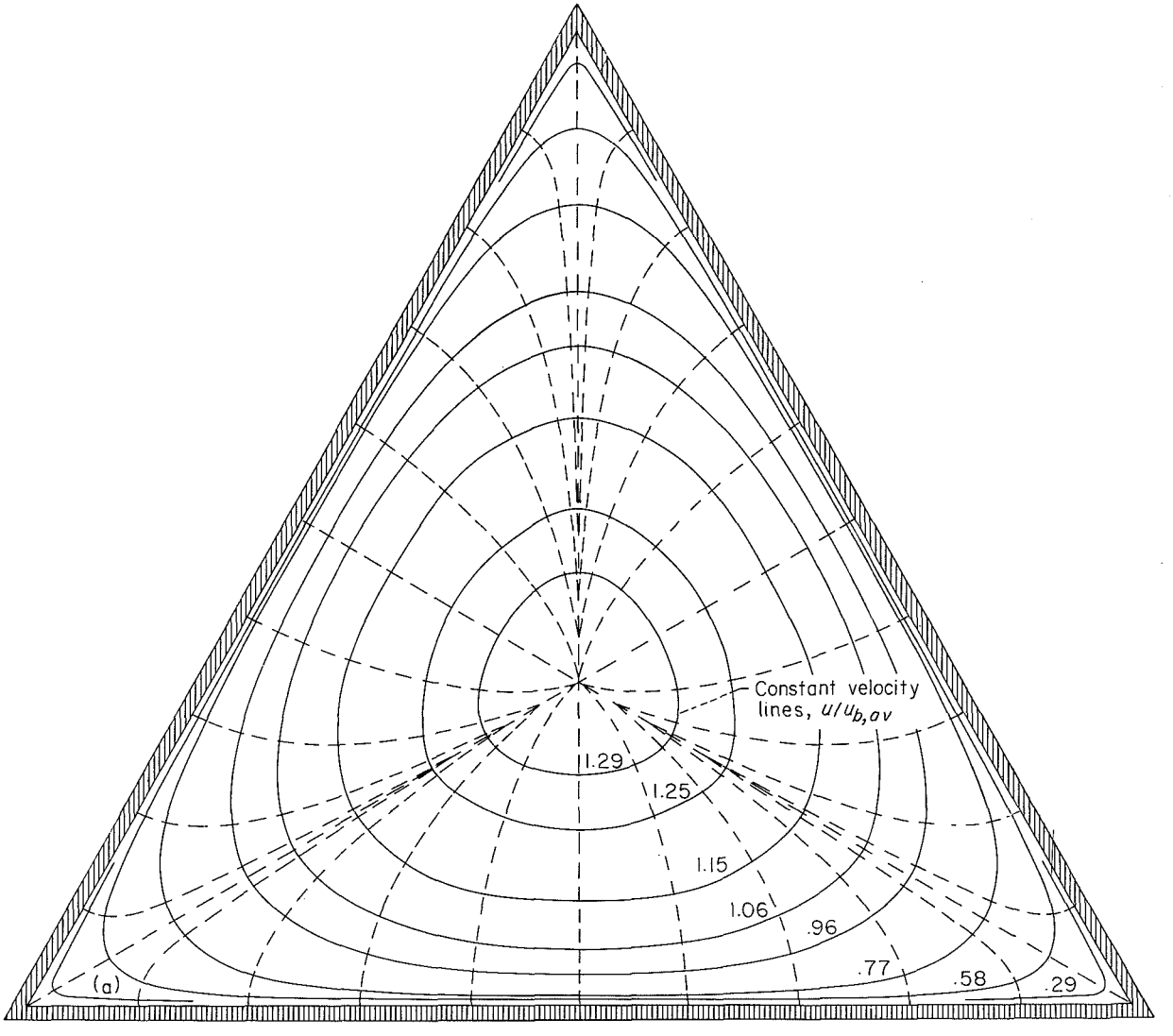

(a) Triangular passage; Reynolds number, 24,000 or 900,000.

FIGURE 3.—Predicted velocity distribution in noncircular passage.

Reynolds number was found to be negligible. In all cases the constant-velocity lines (solid lines) are essentially normal to the velocity-gradient lines (dashed lines) as required. Comparison of these constant-velocity curves and the experimental curves of Nikuradse (ref. 1) indicates that both have the same general shape, although the experimental curves seem to approach the corners more closely than the analytical ones. This might indicate the presence of secondary flows in the corners, as originally suggested by Prandtl, but it appears that no definite conclusions can be drawn on the basis of the available experimental data.

FRICTION FACTOR AND REYNOLDS NUMBER

With the velocity distributions for the passage known, friction factors and Reynolds numbers can be calculated by integrating the distributions to obtain bulk or average velocities. The bulk velocity between two adjacent straight lines normal to the wall (dashed lines in preceding sketch) is first obtained. This bulk velocity varies with position on the tube and is given by

$$u_b \equiv \frac{\int_0^{\Delta A'} u \, dA'}{\Delta A'} \tag{11}$$

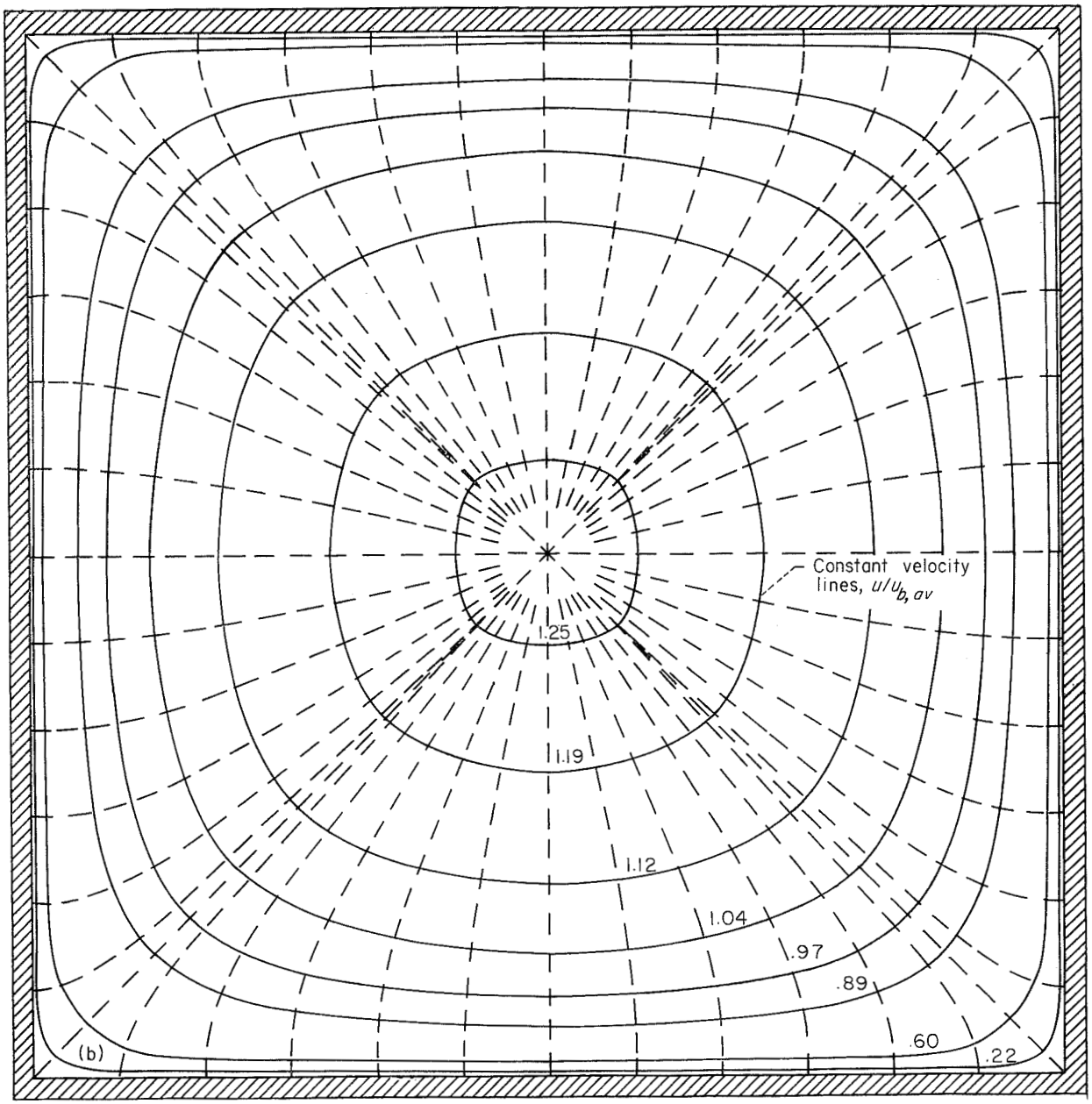

(b) Square passage; Reynolds number, 24,000 or 900,000.

FIGURE 3.—Concluded. Predicted velocity distribution in noncircular passage.

where $\Delta A'$ is the area between two adjacent straight lines normal to the wall. Equation (11) can be written in dimensionless form as

$$u_b^{++}=\frac{\int_0^{\Delta A'} u^{++}\,dA'}{\Delta A} \tag{12}$$

The average velocity for the whole passage is

$$u_{b,av}^{++}=\frac{1}{A}\int_0^A u_b^{++}\,dA \tag{13}$$

where A is the total area of the passage. The variation of $u_b^{++}/u_{b,av}^{++}=u_b/u_{b,av}$ with dimensionless distance from the corner for a low and a high Reynolds number is shown in figure 4.

513554—60——2

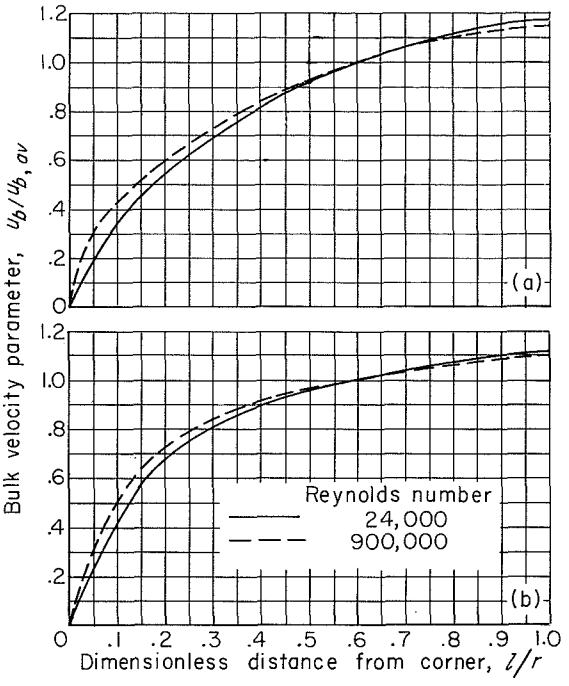

(a) Triangular passage.
(b) Square passage.

FIGURE 4.—Predicted variation of bulk velocity parameter with distance from corner.

For later comparison with heat transfer, the ratio of the local shear stress to the average shear stress can be obtained from equation (9), and corresponding equation for the whole passage, as

$$\frac{\tau_0}{\tau_{0,av}}=\frac{\Delta A}{A}\frac{r}{\Delta l} \tag{14}$$

Curves for $\tau_0/\tau_{0,av}$ against dimensionless distance from the corner are presented in figure 5. The curves indicate that the shear stress is lowest in the region near the corner and goes to zero at the corner. The slopes of the $\tau_0/\tau_{0,av}$ curves near the corners are not as steep as those of Nikuradse; this is probably due to secondary flow in the corners, which is not considered in this analysis. The value of Reynolds number has a small effect on the shape of the curves. The values for the Reynolds numbers were calculated from

$$Re=\frac{u_{b,av}^{++}r^{++}}{r/D_e} \tag{15}$$

which follows directly from the definition of

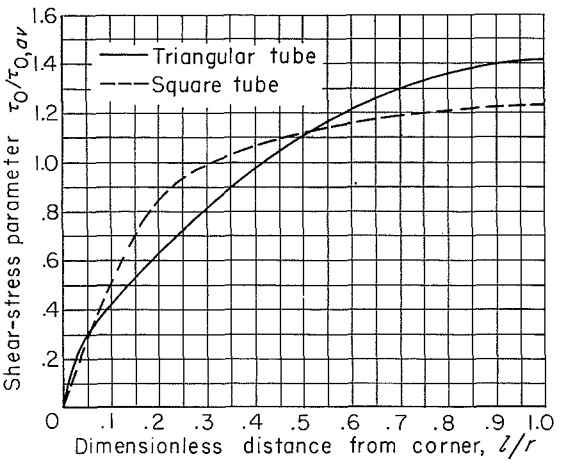

FIGURE 5.—Predicted variation of shear stress on wall with distance from corner. Reynolds number, 24,000 or 900,000.

Reynolds number. The hydraulic diameter D_e is defined in the usual way as four times the flow area over the wetted perimeter.

The fact that the shear stress should decrease in the region near the corner can be seen directly from equation (9), which indicates that the shear stress is proportional to $\Delta A/\Delta l$. But $\Delta A \sim \Delta l y_m$, and hence the shear stress is approximately proportional to y_m, which decreases as the corner is approached.[3]

The friction factor for the passage, based on the pressure gradient, is defined by

$$f\equiv-\frac{D_e\mathrm{d}p/\mathrm{d}x}{2\rho u_{b,av}^2} \tag{16}$$

or, in terms of dimensionless groups,

$$f=\frac{1}{2(r/D_e)u_{b,av}^{++2}} \tag{17}$$

Figures 6 (a) and (b) show friction factors based on the pressure gradient plotted against Reynolds number for the equilateral triangular and the square passages, respectively. Data from reference 10 are included in the figure. The data for the square passage are in good agreement with the predicted curve; those for the triangular passage are about 10 percent above the predicted curve but are still below the circular-tube line taken from reference 7.

[3] It is perhaps surprising that the curves in figure 5 for the triangular passage, as well as those in figure 3(a), have nearly the same shape as corresponding curves calculated for laminar flow.

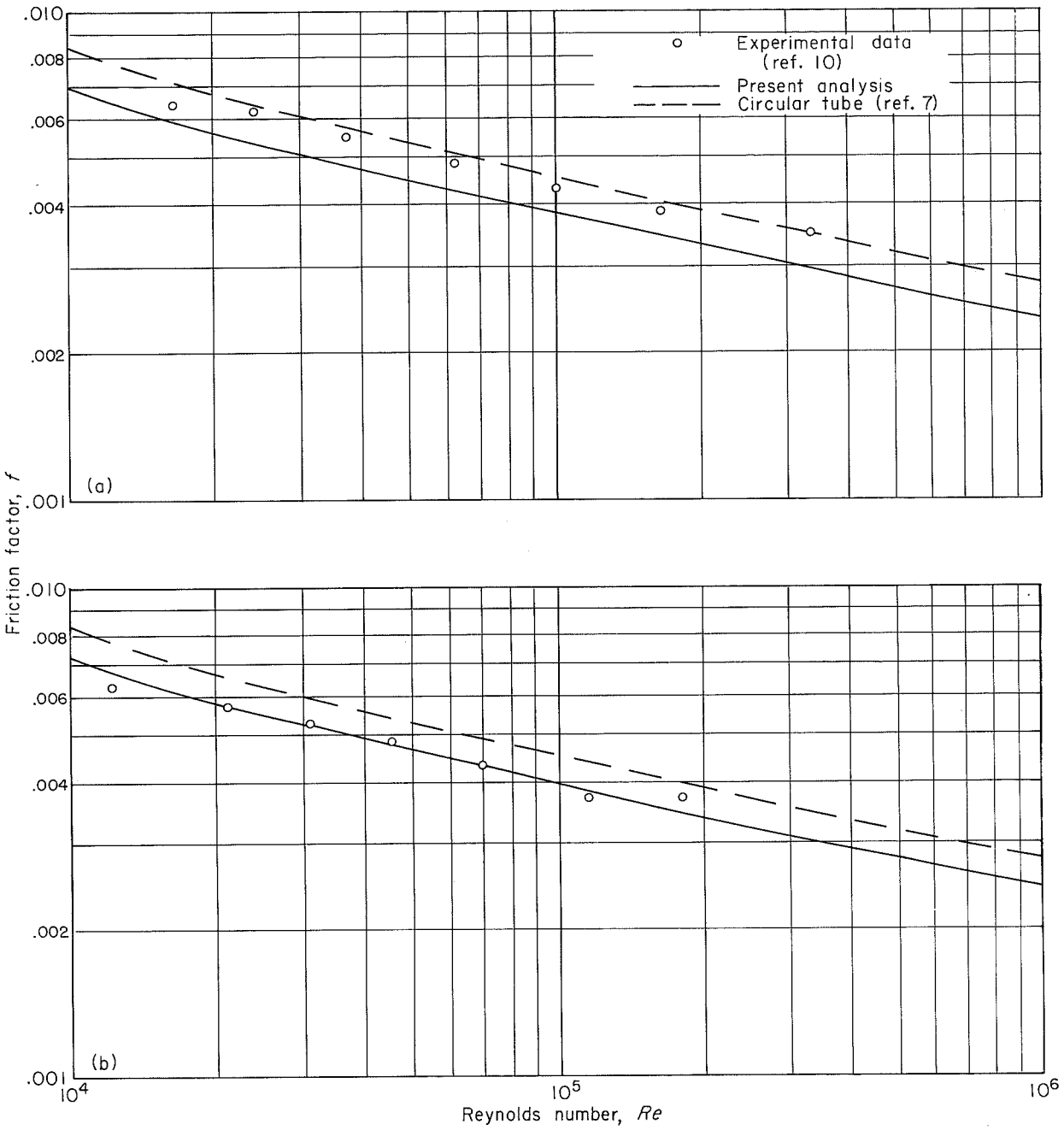

(a) Triangular passage.
(b) Square passage.

FIGURE 6.—Predicted friction factors based on static-pressure gradient as a function of Reynolds number.

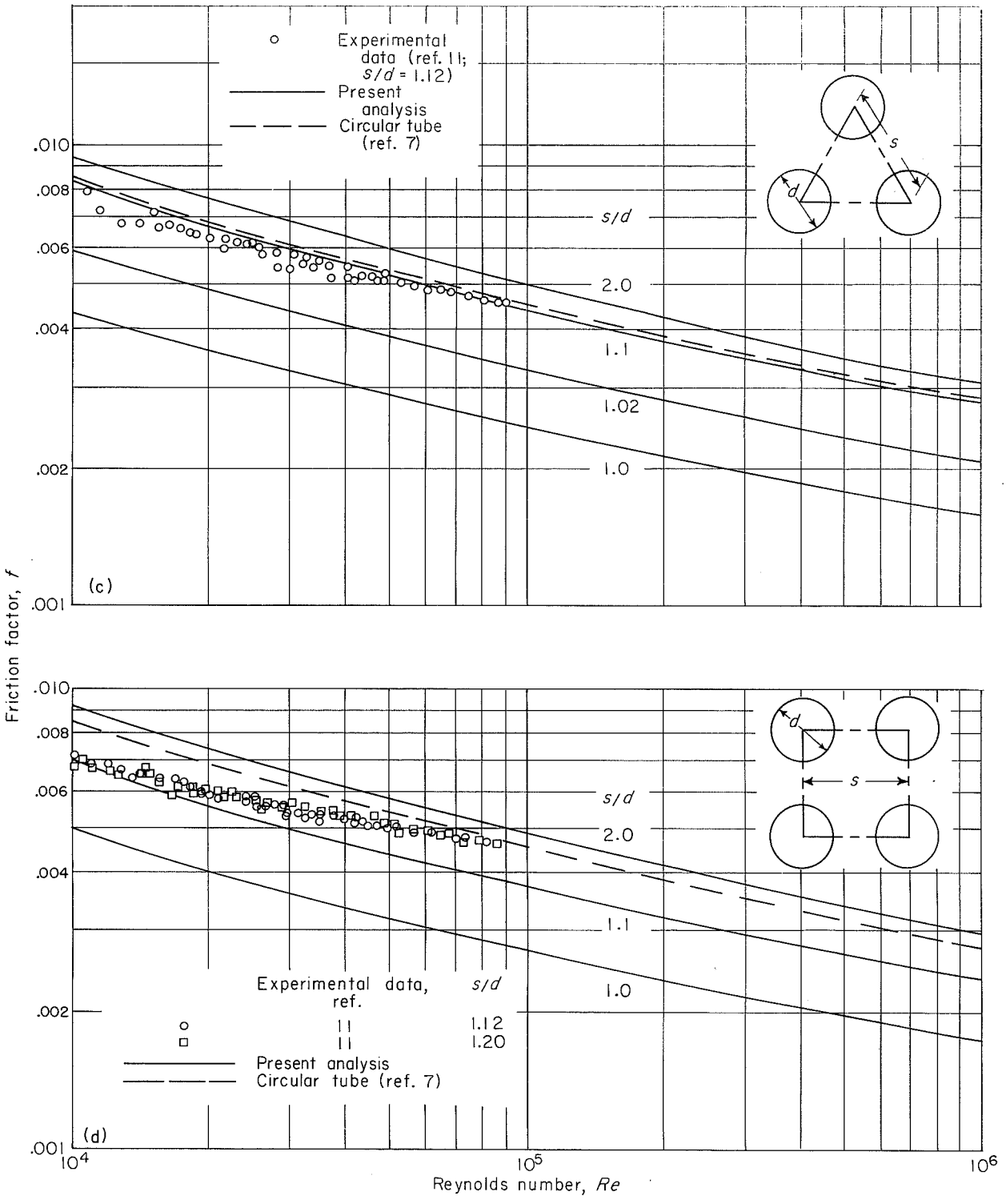

(c) Flow between rods, triangular array.
(d) Flow between rods, square array.

FIGURE 6.—Concluded. Predicted friction factors based on static-pressure gradient as a function of Reynolds number.

Figures 6 (c) and (d) show analytical and experimental friction factors for axial flow between rods. These experimental values (from ref. 11) were not available at the time the analysis for flow between tubes was presented (ref. 3) and so are included herein. The original results in reference 11 have since been recomputed by the authors of that report, and the corrected data are shown in figures 6 (c) and (d). The agreement between analysis and experiment is reasonably good. It is possible that the higher values of the friction factors at the higher Reynolds numbers in the case of the square array are caused by secondary flow. It was found in reference 12 that secondary flows occurred only at the higher Reynolds numbers.

WALL HEAT-TRANSFER DISTRIBUTION

With the velocity distributions previously obtained (and with certain assumptions), the fully developed heat-transfer distributions are calculated herein. From these values, the wall temperature distributions will be calculated in the next section.

The heat added between two straight lines normal to the wall per unit length of tube is $q_0 \Delta l$ (see sketch on p. 5). It is assumed herein that all this heat is used in heating the fluid element between the straight lines. This is a good assumption when the peripheral temperature variation is small compared with the variation of temperature across the passage.

Making a heat balance on the element of fluid between two straight lines normal to the surface and using the foregoing assumption result in [4]

$$q_0 \Delta l = \rho u_b c_p \left(\frac{dt_b}{dx}\right) \Delta A' \tag{18}$$

For the whole passage cross section,

$$q_{0,av} r = \rho u_{b,av} c_p \left(\frac{dt_{b,av}}{dx}\right) A \tag{19}$$

Appendix B shows that, for the fully developed case, $dt_b/dx = dt_{b,av}/dx$ when the heat transfer per unit area at a given circumferential location does not vary with x. Division of equation (18) by equation (19) and conversion to dimensionless form give

$$\frac{q_0}{q_{0,av}} = \frac{u_b^{++}}{u_{b,av}^{++}} \frac{\Delta A}{A} \frac{r}{\Delta l} \tag{20}$$

Equation (20) also gives the ratio of local Nusselt number to average Nusselt number for the case of uniform circumferential wall temperature, when the heat-transfer coefficients are defined in the following way:

$$h = \frac{q_0}{t_0 - t_b} = \frac{q_0}{t_{0,av} - t_{b,av}} \tag{21}$$

and

$$h_{av} = \frac{q_{0,av}}{t_{0,av} - t_{b,av}} \tag{22}$$

or

$$\frac{h}{h_{av}} = \frac{Nu}{Nu_{av}} = \frac{q_0}{q_{0,av}} \tag{23}$$

Equation (23) is true only for the case of uniform circumferential wall temperature, because for any other temperature distribution the temperature differences in equations (21) and (22) will not cancel.

Values of $q_0/q_{0,av}$ (h/h_{av} for uniform circumferential wall temperature) are shown as a function of dimensionless distance from the corner in figure 7.

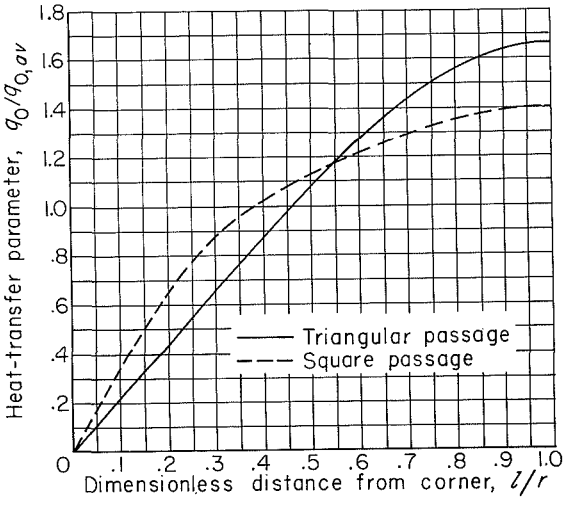

FIGURE 7.—Predicted variation of heat transfer from passage wall with distance from corner. Reynolds number, 24,000 or 900,000.

[4] As an alternative assumption, an element bounded by velocity-gradient lines rather than by straight lines was used. No net heat transfer across the velocity-gradient lines was assumed. This assumption was found to give essentially the same distribution of q_0 as the assumption used in the text.

As was the case with the shear stress (fig. 5), the heat transfer decreases as the corner is approached and goes to zero at the corner. However, comparison of figures 5 and 7 indicates that the heat transfer approaches zero much more rapidly than does the shear stress. Comparison of these figures indicates, therefore, that the assumption of similarity of the shear stress and heat-transfer distributions, which is made in reference 1, might be expected to give heat-transfer coefficients in the vicinity of a corner that are too high. Actually. that assumption gives results that are in reasonable agreement with experiment (ref. 10), possibly because of the compensating effects of secondary flows and peripheral heat transfer in the fluid.

The reason that the heat transfer decreases more rapidly than the shear stress as the corner is approached can easily be seen by comparing equations (9) and (18). Both equations contain $\Delta A/\Delta l$, or $\Delta A'/\Delta l$, which causes the shear stress or heat transfer to decrease near the corner. However, the heat-transfer equation (eq. (18)) contains, in addition, the local bulk velocity u_b, which also decreases; therefore, the heat transfer decreases more rapidly than the shear stress as the corner is approached.

WALL TEMPERATURE DISTRIBUTION

It is assumed in this section that the passage walls are thin and that heat is transferred uniformly to the outside surface of the passages. Uniform heat sources may also be present in the wall. Because of tangential conduction around the wall, the heat transfer through the inner surface will not be uniform and will have the distributions obtained in the preceding section on wall heat transfer. The heat transfer per unit area through the outer surface plus the heat generated per unit volume times the wall thickness is equal to $q_{0,av}$, the average heat transfer per unit area through the inner surface to the fluid.

In order to obtain the temperature distribution around the passage, a heat balance is first made on an element of wall of circumferential length dl. This heat balance gives

$$q_{0,av}-q_0=b\frac{dq_t}{dl} \tag{24}$$

where b is the thickness of the wall and q_t is the tangential heat conduction per unit area. Equation (24) can be written in integral form as

$$\int_0^{l/r}\left(1-\frac{q_0}{q_{0,av}}\right)d\left(\frac{l}{r}\right)=\frac{b}{q_{0,av}r}\int_0^{q_t}dq_t=\frac{b}{q_{0,av}r}q_t \tag{25}$$

where q_t is zero at the corner because the wall temperature distribution is symmetric about that point (temperature gradient is zero). However,

$$q_t=-k_t\frac{dt_0}{dl} \tag{26}$$

Substituting equation (26) in (25) and integrating again result in

$$\int_0^{l/r}\left[\int_0^{l/r}\left(1-\frac{q_0}{q_{0,av}}\right)d\left(\frac{l}{r}\right)\right]d\left(\frac{l}{r}\right)=\frac{k_t b(t_{0,max}-t_0)}{q_{0,av}r^2} \tag{27}$$

where $t_{0,max}$ is the wall temperature at the corner. By using the values of $q_0/q_{0,av}$ obtained in the preceding section, the difference between the maximum wall temperature and the wall temperature at any point for a given heat flux can be calculated from equation (27). A dimensionless parameter containing the difference between the maximum and the average wall temperatures can be obtained by integrating equation (27); that is,

$$\frac{k_t b(t_{0,max}-t_{0,av})}{q_{0,av}r^2}=\int_0^1\frac{k_t b(t_{0,max}-t_0)}{q_{0,av}r^2}d\left(\frac{l}{r}\right) \tag{28}$$

The relation for $k_t b(t_0-t_{0,av})/q_{0,av}r^2$ can be obtained by subtracting equation (27) from (28).

The results for the wall temperature distributions are presented in figure 8, where

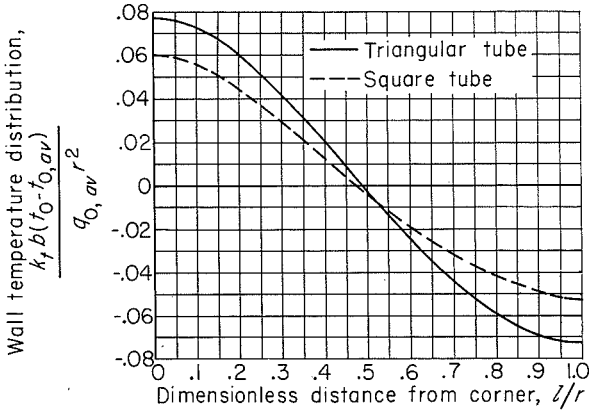

FIGURE 8.—Predicted variation of wall temperature of passage with distance from corner. Reynolds number, 24,000 or 900,000.

$k_t b(t_0-t_{0,av})/q_{0,av}r^2$ is plotted against dimensionless distance from the wall. As mentioned previously, the quantity $q_{0,av}$ in the wall temperature parameter is equal to the sum of the uniform heat flux at the outer wall of the tube and the heat generated per unit volume times the tube wall thickness. Figure 8 indicates that $t_{0,max}-t_{0,av}$, which is the quantity of greatest practical interest, is directly proportional to $q_{0,av}$.

Experimental wall temperature differences from reference 10 were 12 to 60 percent lower than those in figure 8. This difference might be caused by secondary flows or by peripheral conduction and turbulent transport in the fluid, both of which were neglected in the analysis, or by nonuniform heat generation in the test-section walls.

AVERAGE HEAT-TRANSFER COEFFICIENTS

All the results obtained thus far (wall heat-transfer distributions, wall temperature distributions, etc.) were independent of Prandtl number, inasmuch as it was not necessary to use the generalized temperature distribution in figure 2. However, it is necessary to use that distribution for obtaining the difference between wall and bulk temperatures that corresponds to a given heat flow, that is, for obtaining the heat-transfer coefficient.

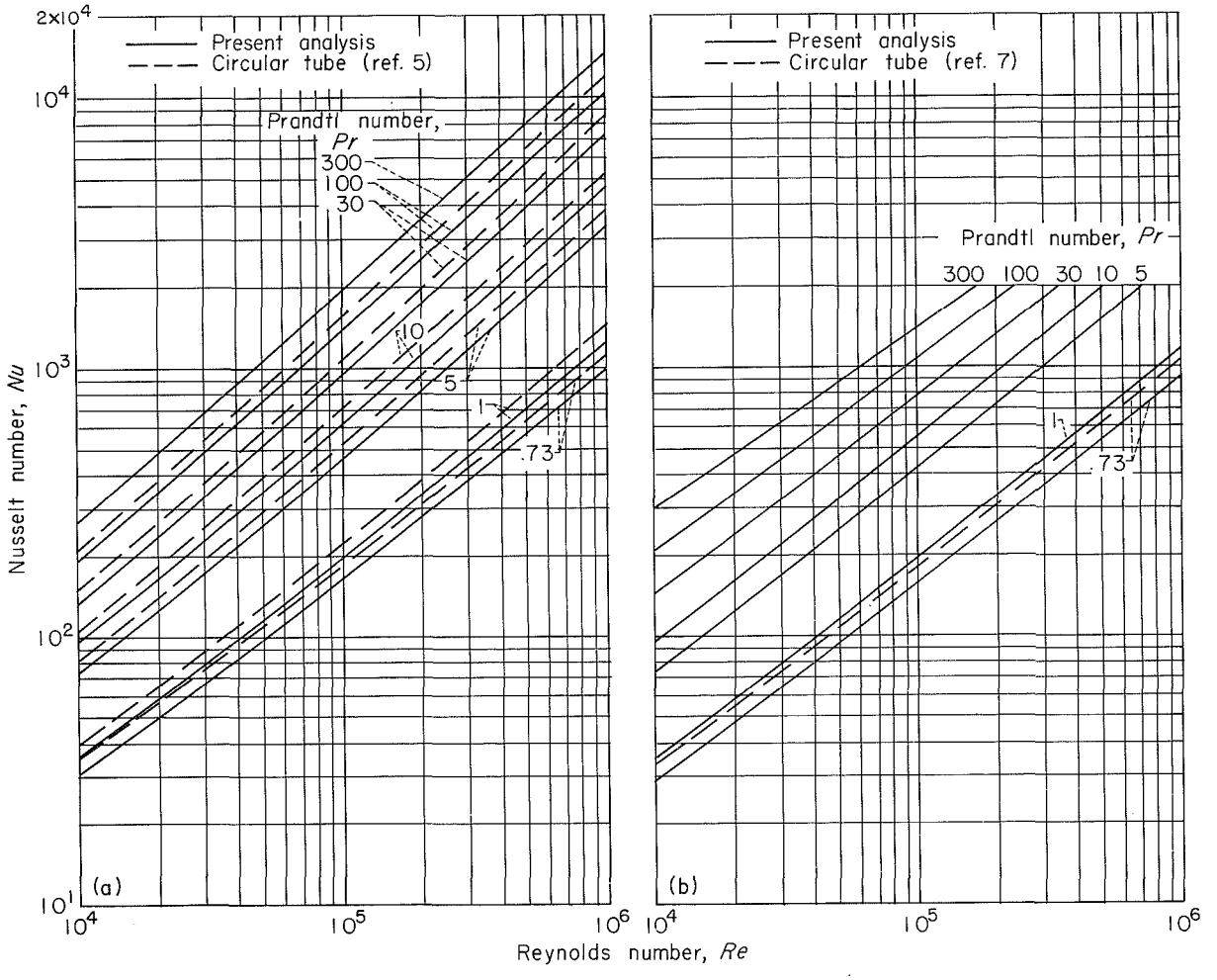

(a) Triangular passage, $\frac{kr}{k_t b}=0$ (uniform peripheral wall temperature distribution).

(b) Triangular passage, $\frac{kr}{k_t b}=0.005$ (nonuniform peripheral wall temperature distribution).

FIGURE 9.—Predicted average Nusselt number as a function of Reynolds number and Prandtl number.

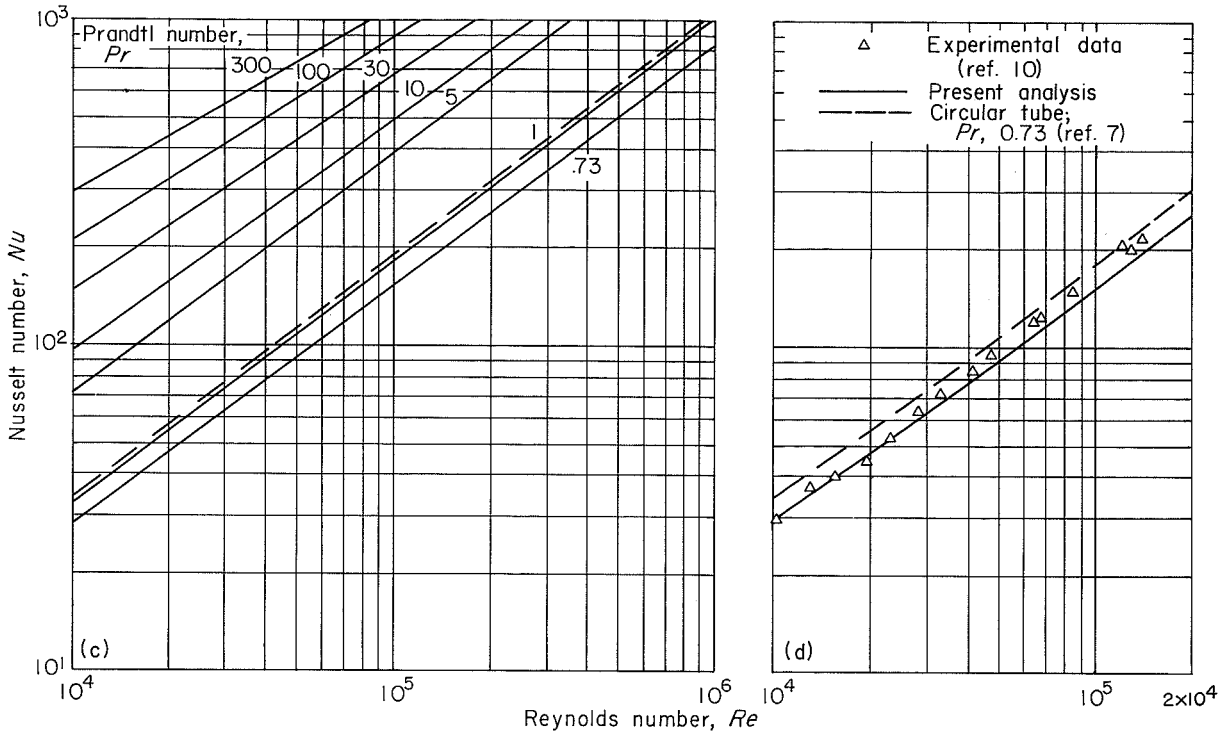

(c) Triangular passage, $\frac{kr}{k_t b}=0.010$ (nonuniform peripheral wall temperature distribution).

(d) Triangular passage, $\frac{kr}{k_t b}=0.025$ (nonuniform peripheral wall temperature distribution).

FIGURE 9.—Continued. Predicted average Nusselt number as a function of Reynolds number and Prandtl number.

The average heat-transfer coefficient for the inner wall of the passage is defined by

$$h_{av}\equiv\frac{q_{0,av}}{t_{0,av}-t_{b,av}} \tag{29}$$

where

$$t_{0,av}=\int_0^1 t_0\,\mathrm{d}\left(\frac{l}{r}\right) \tag{30}$$

$$t_b=\frac{\int_0^{\Delta A'} tu\,\mathrm{d}A}{u_b\Delta A'} \tag{31}$$

and

$$t_{b,av}=\frac{\int_0^{A_0} t_b u_b\,\mathrm{d}A}{u_{b,av}A_0} \tag{32}$$

The average Nusselt number corresponding to the average heat-transfer coefficient (eq. (29)) can be calculated from the following equation, which can be verified by substituting the definitions of the various quantities:

$$\frac{1}{Nu_{av}}=\frac{r/De}{r^{++}Pr}\int_0^1\frac{q_0}{q_{0,av}}t_b^{++}\left(\frac{v'_b}{u_{b,av}}\right)\mathrm{d}\left(\frac{A}{A_0}\right)-\frac{r}{D_e}\frac{kr}{k_t b}\int_0^1\frac{k_t b(t_0-t_{0,av})}{q_{0,av}r^2}\left(\frac{v'_b}{u_{b,av}}\right)\mathrm{d}\left(\frac{A}{A_0}\right) \tag{33}$$

where

$$t_b^{++}=\int_0^1 t^{++}\frac{u^{++}}{u_b^{++}}\,\mathrm{d}\left(\frac{A}{\Delta A}\right) \tag{34}$$

and

$$t^{++}=\frac{t^+r^{++}y_m/r}{y_m^+} \tag{35}$$

As in the case of velocity distributions, the values of y^+ are measured along lines that are normal to the wall and extend to the line of maximum velocities. The values of t^+ are obtained from figure 2.

Average Nusselt numbers calculated by equation (33) are plotted against Reynolds number for various values of the parameter $kr/k_t b$ and of Prandtl number in figure 9. The parameter $kr/k_t b$ is zero for uniform wall temperature and increases as the variation of wall temperature

increases. The wall temperature distributions were obtained from figure 8. The Nusselt numbers decrease as $kr/k_t b$ increases or as tube conductivity or thickness decreases; that is, the Nusselt numbers decrease as the wall temperature variation increases. These trends are qualitatively similar to those obtained for laminar flow in reference 13, where it was found that the Nusselt number for a rectangular duct with uniform peripheral heat flux was lower than that for uniform wall temperature.

Experimental data from reference 10 are included in figures 9(d) and (h). In general, the data are in reasonably good agreement with the predicted values. It is possible that the slight departure from the predicted curves at the higher Reynolds numbers is caused by secondary flow (ref. 12).

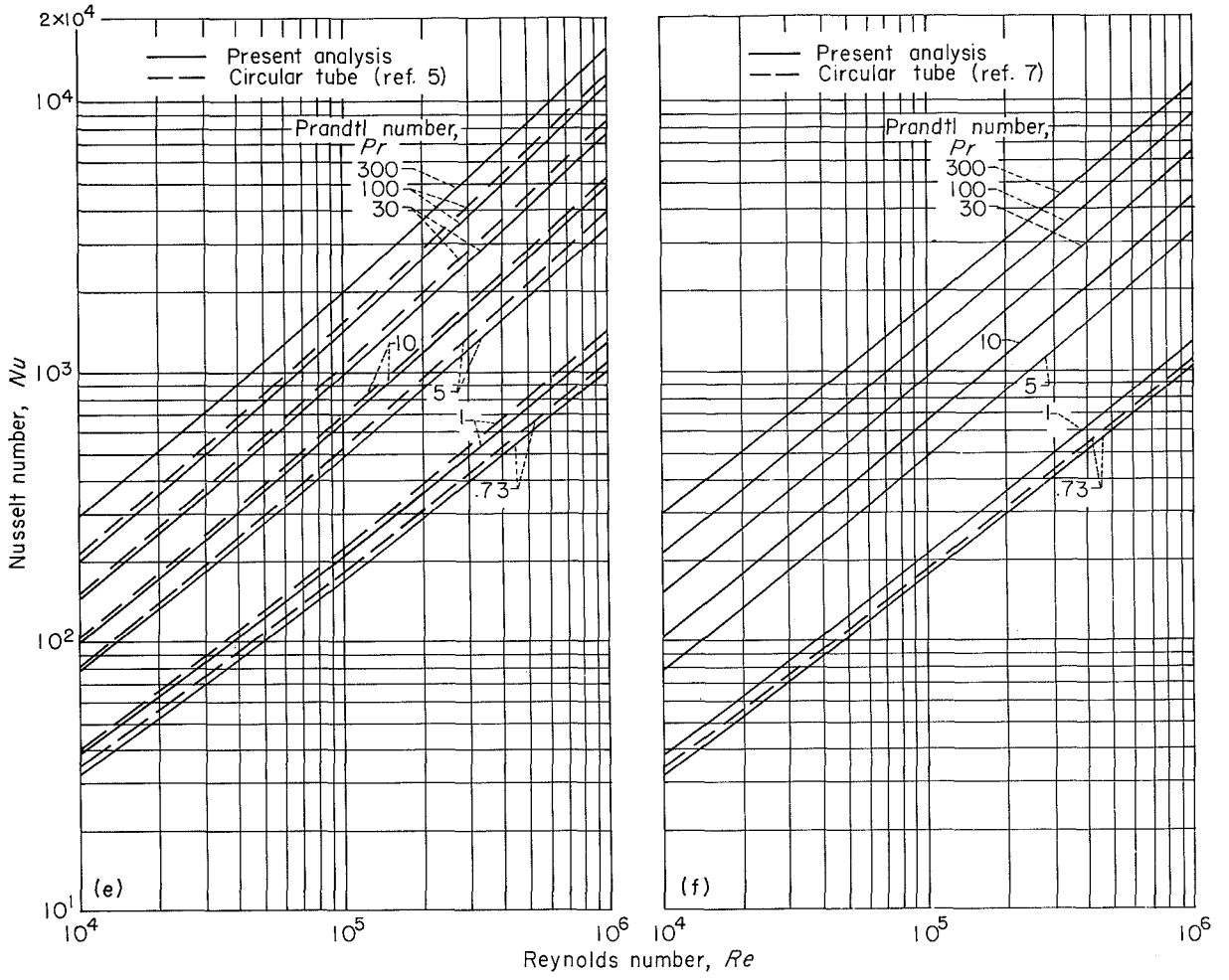

(e) Square passage, $\frac{kr}{k_t b}=0$ (uniform peripheral wall temperature distribution).

(f) Square passage, $\frac{kr}{k_t b}=0.005$ (nonuniform peripheral wall temperature distribution).

FIGURE 9.—Continued. Predicted average Nusselt number as a function of Reynolds number and Prandtl number.

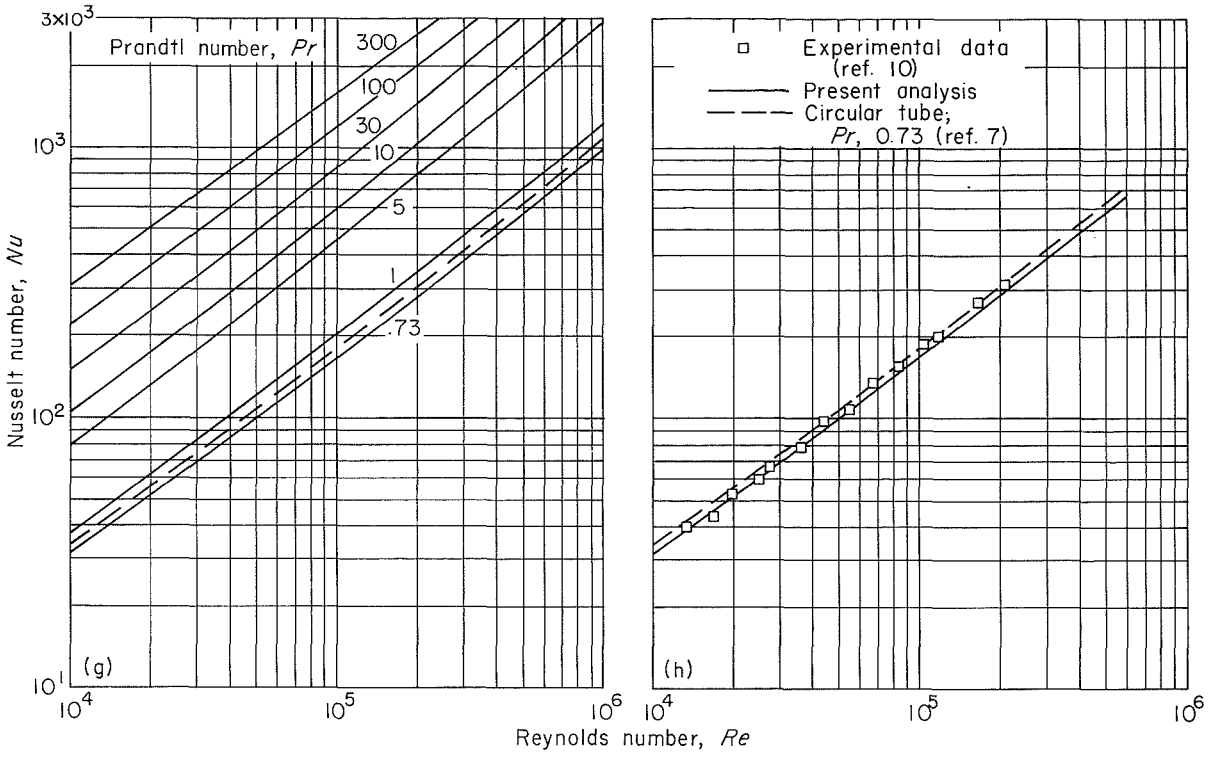

(g) Square passage, $\frac{kr}{k_t b}=0.010$ (nonuniform peripheral wall temperature distribution).

(h) Square passage, $\frac{kr}{k_t b}=0.015$ (nonuniform peripheral wall temperature distribution).

FIGURE 9.—Concluded. Predicted average Nusselt number as a function of Reynolds number and Prandtl number.

SUMMARY OF RESULTS

The following results were obtained from the analytical investigation of fully developed axial turbulent flow in noncircular passages with heat transfer:

1. The velocities and shear stresses in the region near the corner were lower than the average values and went to zero at the corner.

2. When the passages were heated, the heat transfer to the fluid in the region near the corner was lower than the average value and went to zero at the corner.

3. The friction factors for the noncircular passages were somewhat lower than those for a circular tube.

4. When uniform heat sources in the passage wall and uniform heat transfer at the surface were assumed to occur, the difference between the maximum and average wall temperatures was directly proportional to the heat flux.

5. The average Nusselt numbers for the noncircular passages were somewhat lower than those for a circular tube. The average Nusselt number was also found to be a function of wall temperature distribution and of Prandtl number.

LEWIS RESEARCH CENTER
NATIONAL AERONAUTICS AND SPACE ADMINISTRATION
CLEVELAND, OHIO, *August 21, 1958*

APPENDIX A

SYMBOLS AND DIMENSIONLESS QUANTITIES

A	area
A_0	total area of section of passage
b	wall thickness of passage
c_p	specific heat of fluid at constant pressure
D_e	equivalent diameter
f	friction factor, $\dfrac{-D_e \dfrac{dp}{dx}}{2\rho u_{b,av}^2}$
h	local heat-transfer coefficient, $\dfrac{q_0}{t_0 - t_{b,av}}$
h_{av}	average heat-transfer coefficient, $\dfrac{q_{0,av}}{t_{0,av} - t_{b,av}}$
k	thermal conductivity of fluid
k_t	thermal conductivity of material of passage wall
$\dfrac{k_t b (t_0 - t_{0,av})}{q_{0,av} r^2}$	wall temperature distribution
l	peripheral distance along the wall from corner
Nu	Nusselt number based on local heat transfer, hD_e/k
Nu_{av}	Nusselt number based on average heat transfer, $h_{av}D_e/k$
n	constant, 0.124
Pr	Prandtl number, $c_p\mu/k$
p	static pressure
q	rate of heat transfer per unit area
q_0	rate of heat transfer from wall of passage per unit area
$q_{0,av}$	average rate of heat transfer from wall of passage per unit area
Re	Reynolds number, $\rho u_b D_e/\mu$
r	distance from corner to midpoint of wall
r^{++}	parameter, $\dfrac{\sqrt{\dfrac{-r(dp/dx)}{\rho}}}{\mu\rho} r$
t	temperature of fluid at a point
t^+	temperature parameter, $\dfrac{(t_0 - t)c_p\tau_0}{q_0\sqrt{r/\rho}}$
t^{++}	temperature parameter, $\dfrac{(t_0 - t)c_p\rho\sqrt{\dfrac{-r(dp/dx)}{\rho}}}{q_0}$
t_a	arbitrary temperature at a given cross section
t_b	local bulk temperature of fluid at given distance from corner at cross section of flow passage
t_b^{++}	bulk-temperature parameter, $\displaystyle\int_0^1 t_b^{++} \frac{u^{++}}{u_b^{++}} d\left(\frac{A}{\Delta A}\right)$
t_0	wall temperature
$t_{0,max}$	maximum wall temperature of passage
u	time-average velocity parallel to wall at a point
u^+	velocity parameter, $u/\sqrt{\tau_0/\rho}$
u^{++}	velocity parameter, $\dfrac{u}{\sqrt{\dfrac{-r(dp/dx)}{\rho}}}$
u_b	local bulk velocity at given distance from corner at cross section of flow passage
u_b^{++}	bulk-velocity parameter, $\dfrac{\displaystyle\int_0^{\Delta A} u\, dA}{\Delta A}$
$u_{b,av}^{++}$	bulk-velocity parameter, $\dfrac{1}{A}\displaystyle\int_0^A u_b\, dA$
x	axial distance along passage
y	normal distance from wall
y^+	wall distance parameter, $\dfrac{\sqrt{\tau_0/\rho}}{\mu/\rho} y$
y_m	value of y at $u = u_m$
y_m^+	y^+ evaluated at line of maximum velocities
α	ratio of eddy diffusivity for heat transfer to eddy diffusivity for momentum transfer, ϵ_h/ϵ
ϵ	coefficient of eddy diffusivity for momentum
ϵ_h	coefficient of eddy diffusivity for heat
κ	Kármán constant, 0.36
μ	absolute viscosity of fluid
ν	kinematic viscosity
ρ	mass density of fluid
τ	shear stress in fluid

Subscripts:

av	average
t	tangential
0	pertaining to a wall

APPENDIX B

CONDITION FOR FULLY DEVELOPED HEAT TRANSFER

For fully developed heat transfer and constant fluid properties,

$$\frac{q_0}{t_0-t_a}=h_a \tag{B1}$$

where h_a, an arbitrary heat-transfer coefficient, is independent of x. If h_a were not independent of x at a great distance from the entrance (cyclic variations of h_a excluded), the absolute value of h_a would become arbitrarily large as x increased, so that for finite temperature differences the absolute value of q_0 would become arbitrarily large. The following equations are special cases of equation (B1):

$$\frac{q_0}{t_0-t_{b,av}}=h \tag{B2}$$

$$\frac{q_0}{t_0-t_b}=h \tag{B3}$$

For the case where the wall heat transfer per unit area is independent of x (but not of circumferential position), equations (B2) and (B3) can be differentiated to give the following results:

$$\frac{dt_0}{dx}=\frac{dt_{b,av}}{dx}$$

$$\frac{dt_0}{dx}=\frac{dt_b}{dx}$$

or

$$\frac{dt_b}{dx}=\frac{dt_{b,av}}{dx}$$

The quantity dt_b/dx is therefore independent of circumferential position when the heat transfer is independent of x.

REFERENCES

1. Eckert, E. R. G., and Low, George M.: Temperature Distribution in Internally Heated Walls of Heat Exchangers Composed of Noncircular Flow Passages. NACA Rep. 1022, 1951. (Supersedes NACA TN 2257.)
2. Elrod, Harold G., Jr.: Turbulent Heat Transfer in Polygonal Flow Sections. NDA–10–7, Nuclear Dev. Associates, Inc. (New York), Sept. 22, 1952.
3. Deissler, Robert G., and Taylor, Maynard F.: Analysis of Axial Turbulent Flow and Heat Transfer Through Banks of Rods or Tubes. TID–7529, Reactor Heat Transfer Conf., pt. 1, book 1, Nov. 1957, pp. 416–461.
4. Deissler, Robert G., and Taylor, Maynard F.: Analysis of Fully Developed Turbulent Heat Transfer and Flow in an Annulus with Various Eccentricities. NACA TN 3451, 1955.
5. Deissler, Robert G.: Analysis of Turbulent Heat Transfer, Mass Transfer, and Friction in Smooth Tubes at High Prandtl and Schmidt Numbers. NACA Rep. 1210, 1955. (Supersedes NACA TN 3145.)
6. Deissler, Robert G.: Analytical and Experimental Investigation of Adiabatic Turbulent Flow in Smooth Tubes. NACA TN 2138, 1950.
7. Deissler, R. G., and Eian, C. S.: Analytical and Experimental Investigation of Fully Developed Turbulent Flow of Air in a Smooth Tube with Heat Transfer with Variable Fluid Properties. NACA TN 2629, 1952.
8. Deissler, R. G.: Analysis of Fully Developed Turbulent Heat Transfer at Low Peclet Numbers in Smooth Tubes with Application to Liquid Metals. NACA RM E52F05, 1952.
9. Laufer, John: The Structure of Turbulence in Fully Developed Pipe Flow. NACA Rep. 1174, 1954. (Supersedes NACA TN 2954.)
10. Lowdermilk, Warren H., Weiland, Walter F., Jr., and Livingood, John N. B.: Measurement of Heat-Transfer and Friction Coefficients for Flow of Air in Noncircular Ducts at High Surface Temperatures. NACA RM E53J07, 1954.
11. LeTourneau, B. W., Grimble, R. E., and Zerbe, J. E.: Pressure Drop for Parallel Flow Through Rod Bundles. Preprint No. 56–A–134, ASME, 1956.
12. Eckert, E. R. G., and Irving, T. F., Jr.: Flow in Corners of Passages with Noncircular Cross Sections. Trans. ASME, vol. 78, no. 4, May 1956, pp. 709–718.
13. Sparrow, E. M., and Siegel, R.: A Variational Method for Fully-Developed Laminar Heat Transfer in Ducts. Trans. ASME (Jour. Heat Transfer), ser. c, vol. 81, no. 2, May 1959, pp. 157–167.

U.S. GOVERNMENT PRINTING OFFICE: 1960